Supplementary Information

Evaluation methods of adsorbents for air purification and gas separation at low concentration. Case studies on xenon and krypton.

Arnaud Monpezat,[a] Sylvain Topin,[a,] Ludovic Deliere,[a] David Farrusseng,[b,]* Benoit Coasne [c,]**

[a] CEA, DAM, DIF, F-91297 Arpajon – Cedex, France

[b] Université de Lyon, Université Claude Bernard Lyon 1, CNRS, IRCELYON - UMR 5256, 2 Avenue Albert Einstein, 69626 Villeurbanne Cedex, France

[c] Univ. Grenoble Alpes, CNRS, LIPhy, 38000 Grenoble, France

*** Corresponding Author**

Sylvain Topin (sylvain.topin@cea.fr)

David Farrusseng (david.farrusseng@ircelyon.univ-lyon1.fr)

Benoit Coasne (benoit.coasne@univ-grenoble-alpes.fr)

Table S1. Adsorption properties of the different adsorbents.

Material	Specific area (m^2/g)	Pores / cages (Å)	Porosity (%)	Porous volume (cm^3/g)	Grain size (µm)	Silver content & nanoparticles size (nm)	Stability	Preparation	Ref.
AC	1000				300 - 500			Purchased at MERCK© (Charcoal activated for gas chromatography) Engineered particles	††
Ni-MOF-74	500	11		0.27 – 0.77			hydrothermal stability		[1,2]
CC3	550	4.4					hydrothermal stability		[3,4]
Co-formate	300	5					hydrothermal stability		[5]
HKUST-1	692 - 1710	5 and 15		0.333 and 0.8			sensitive to humidity		[6–10]
SBMOF-1	145	4.2	16				thermal (until 500 K) stability		[11,12]
SBMOF-2	195	6.34 and 6.66	25.6						[12,13]
Noria	350	3.6-8		0.13			thermal stability		[14,15]
Ag@ZSM-5	BET : 311 t-plot : 415	5.5		BET : 0.186 t-plot : 0.118 (micropore volume)	315 – 500 †	9 %wt † 3 nm †	thermal stability	Na@ZSM-5 purchased from TOSOH© Silver exchanged Engineered particles (pressed and sieved)	[16–18], †
Ag@ETS-10	BET : 232 † t-plot : 310 †	~8		BET : 0.141 t-plot : 0.0784 † (micropore volume)	200 – 1000 †	30 %wt > 5 nm †		Purchased at EXTRAORDINARY ADSORBENT INC, Canada Engineered particles	[19], †

† *This work*

†† *Material datasheet*

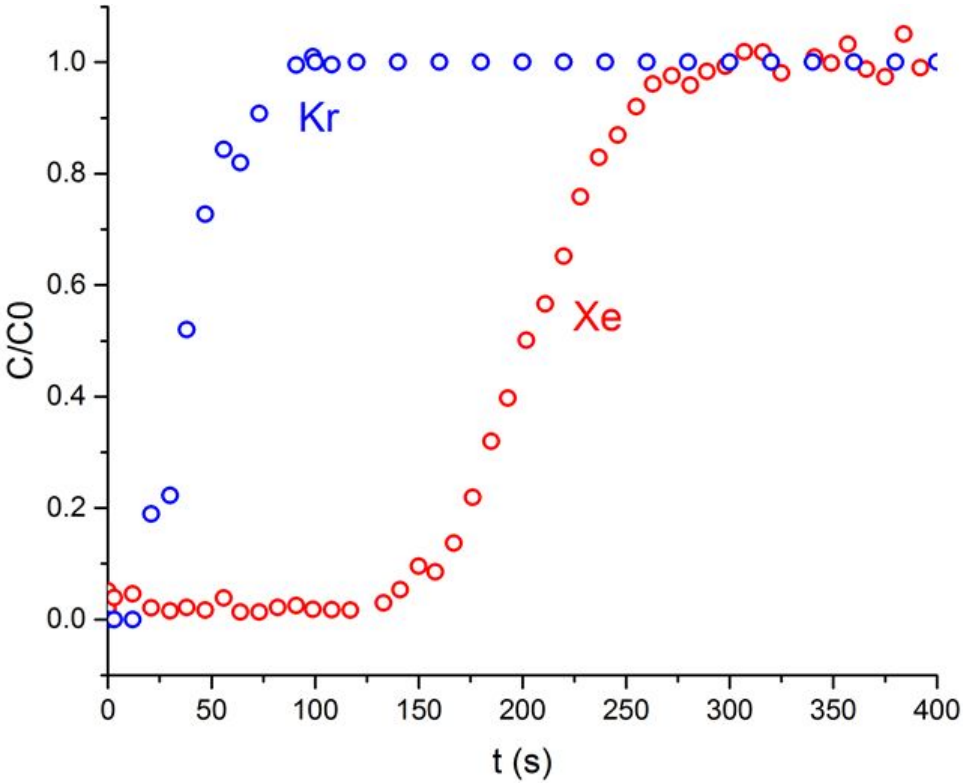

Figure S1. 1 ppm Xe (○) and 1 ppm Kr (○) in air breakthrough curves at 298 K for the activated carbon (gasflow = 60 mL/min ; mass of adsorbent = 0.2931 g).

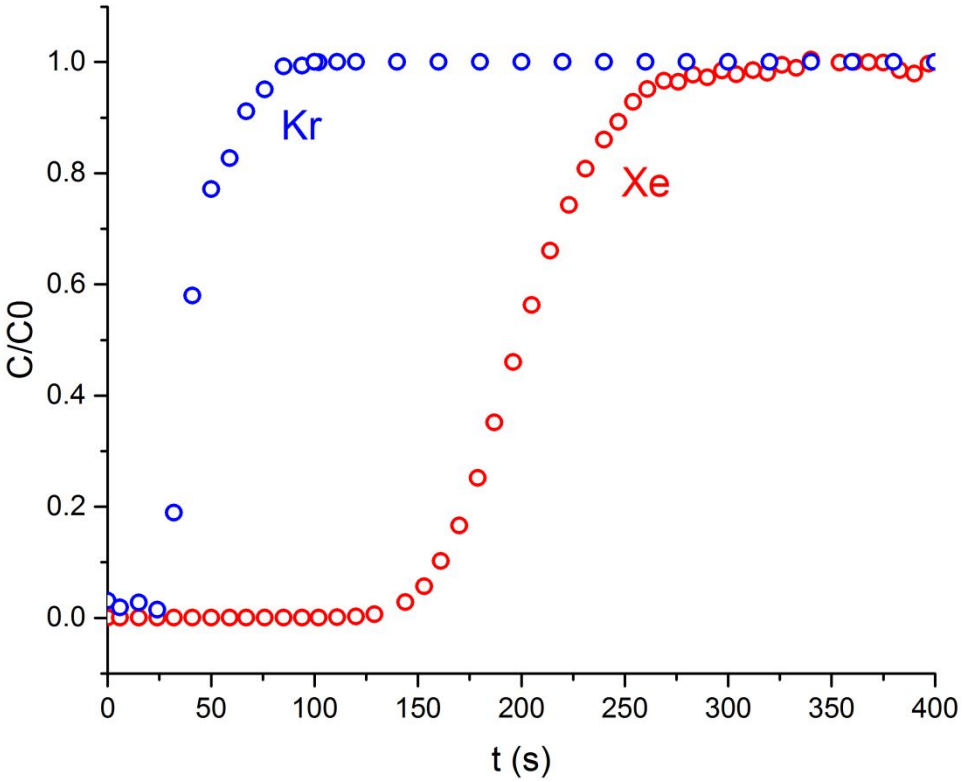

Figure S2. 400 ppm Xe (○) and 40 ppm Kr (○) in air breakthrough curves at 298 K for the activated carbon (gasflow = 60 mL/min ; mass of adsorbent = 0.2931 g)

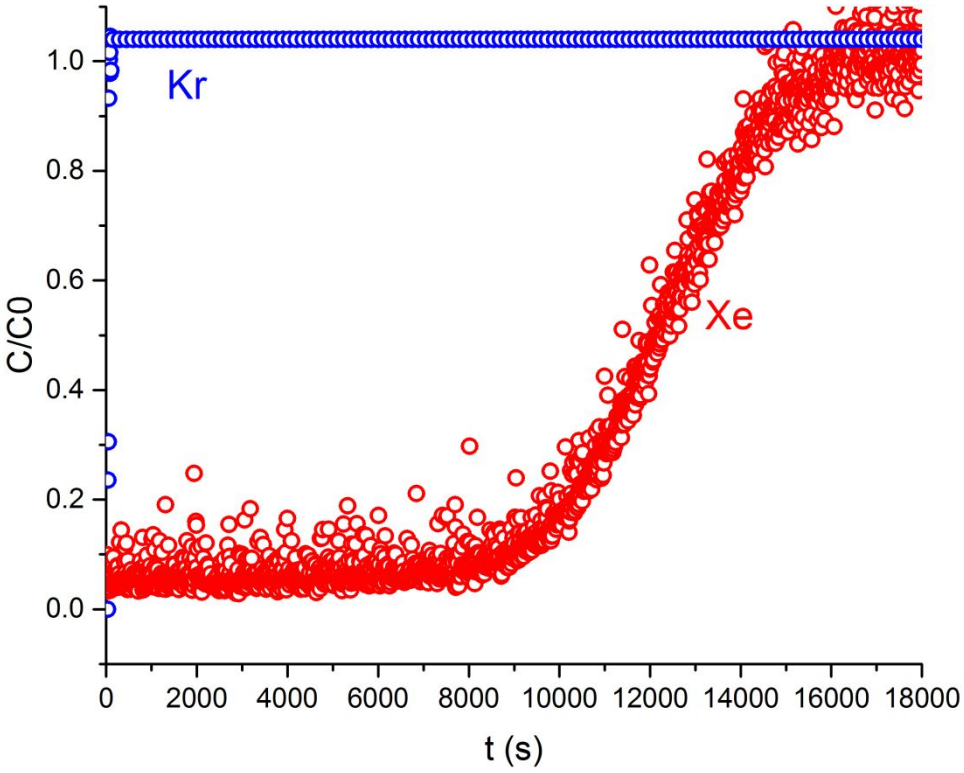

Figure S3. 1 ppm Xe (O) and 1 ppm Kr (O) in air breakthrough curves at 298 K for the Ag@ZSM-5 (gasflow = 60 mL/min ; mass of adsorbent = 0.3815 g)

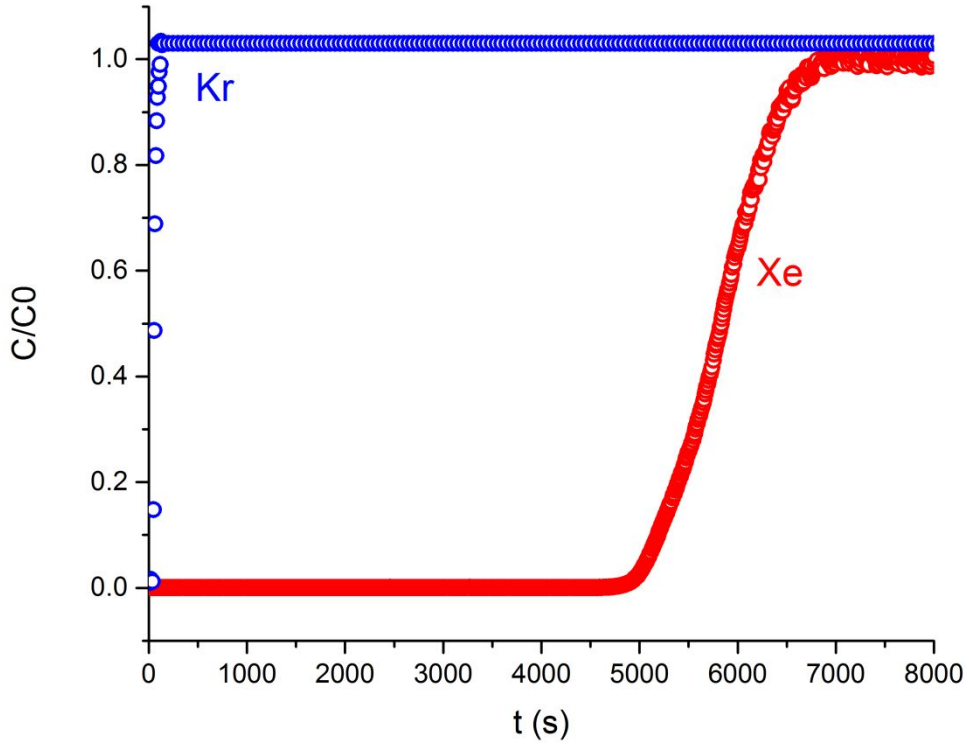

Figure S4. 400 ppm Xe (O) and 40 ppm Kr (O) in air breakthrough curves at 298 K for the Ag@ZSM-5 (gasflow = 60 mL/min ; mass of adsorbent = 0.3815 g)

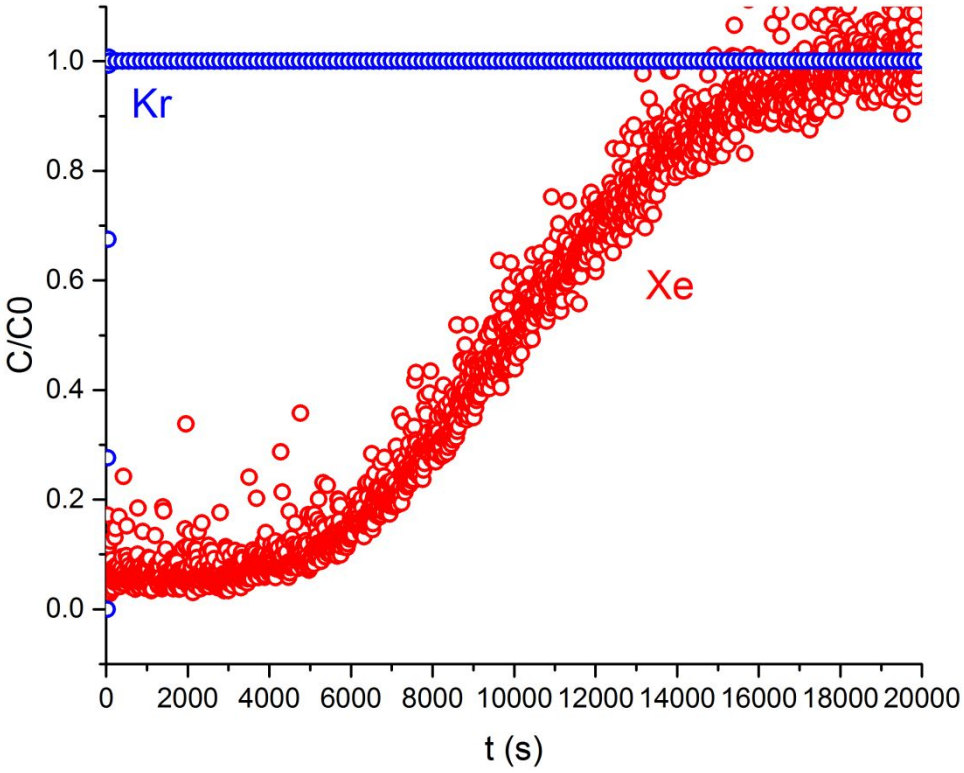

Figure S5. 1 ppm Xe (○) and 1 ppm Kr (○) in air breakthrough curves at 298 K for the Ag@ETS-10 (gasflow = 60 mL/min ; mass of adsorbent = 0.3907 g)

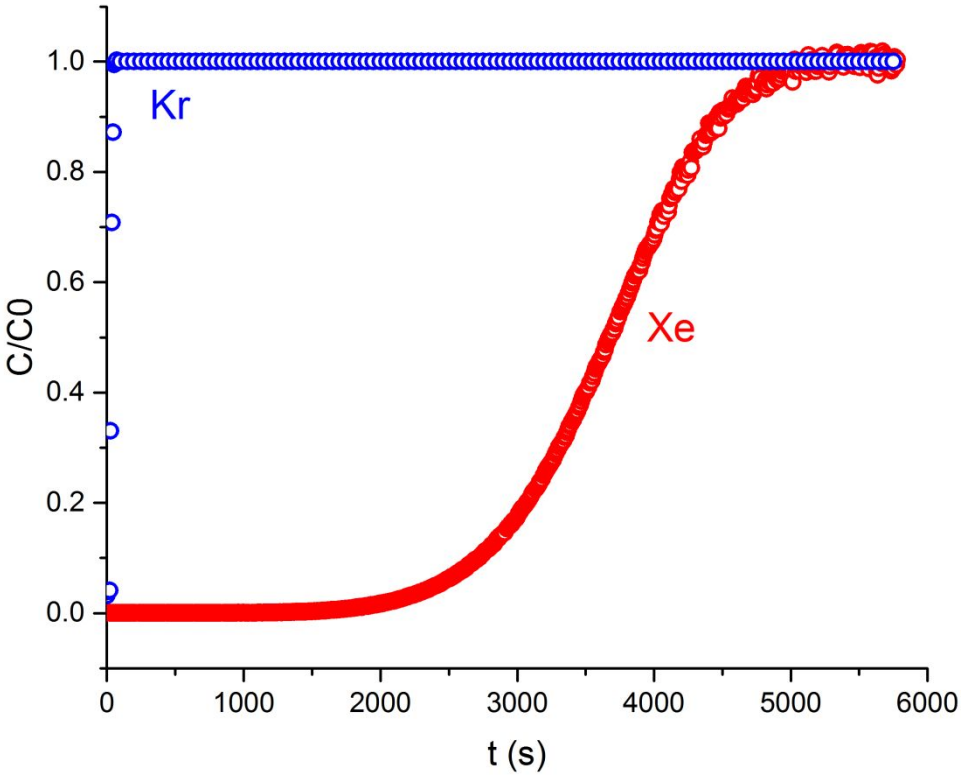

Figure S6. 400 ppm Xe (O) and 40 ppm Kr (O) in air breakthrough curves at 298 K for the Ag@ETS-10 (gasflow = 60 mL/min ; mass of adsorbent = 0.3907 g)

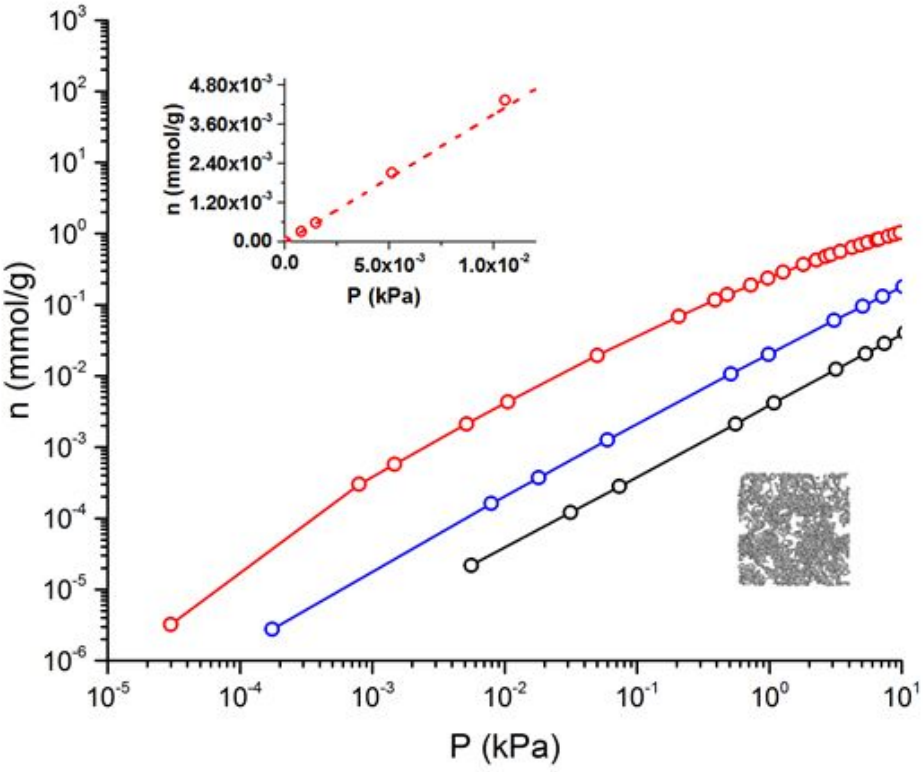

Figure. S7. Experimental Adsorption isotherms at 298 K of Xe (O), Kr (O) and N2 (O) on Activate Carbon ; (insert) the first points of the xenon adsorption isotherm and the linear fit for the determination of the Henry coefficient.

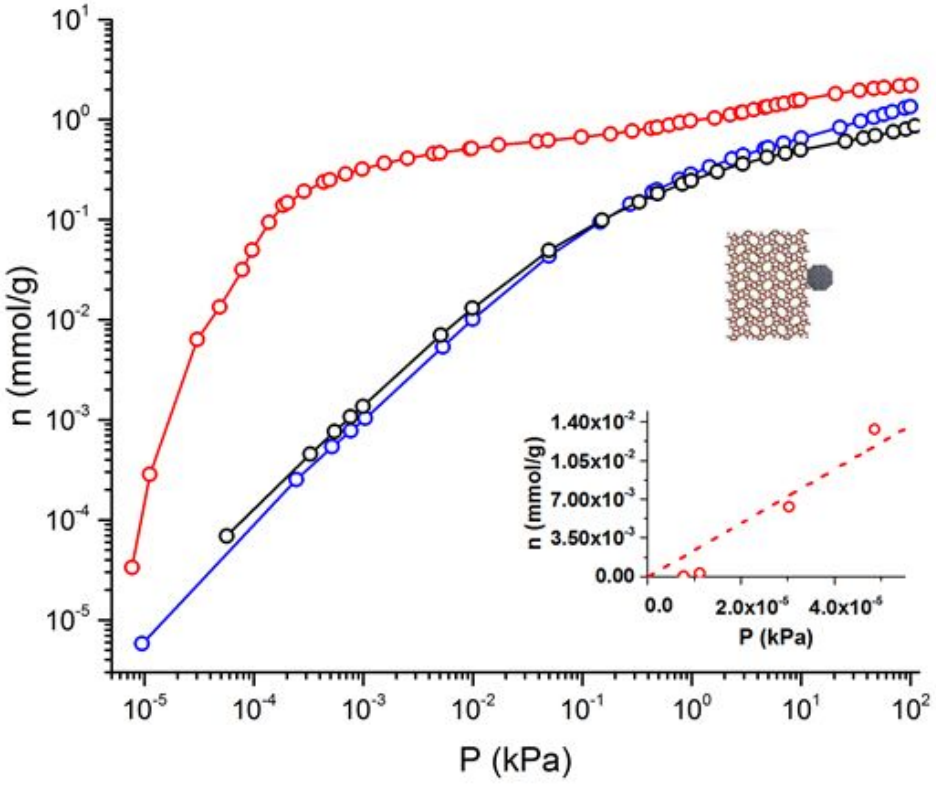

Figure S8. Experimental Adsorption isotherms at 298 K of Xe (O), Kr (O) and N2 (O) on Ag@ZSM-5 ; (insert) the first points of the xenon adsorption isotherm and the linear fit for the determination of the Henry coefficient.

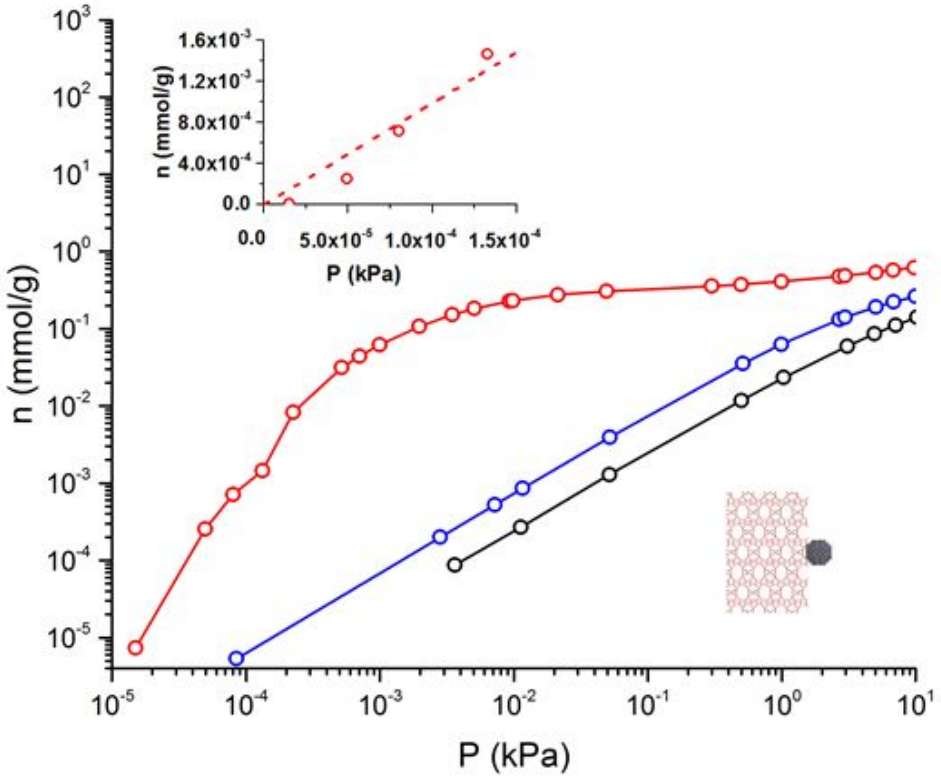

Figure S9. Experimental Adsorption isotherms at 298 K of Xe (○), Kr (○) and N2 (○) on Ag@ETS-10 ; (insert) the first points of the xenon adsorption isotherm and the linear fit for the determination of the Henry coefficient.

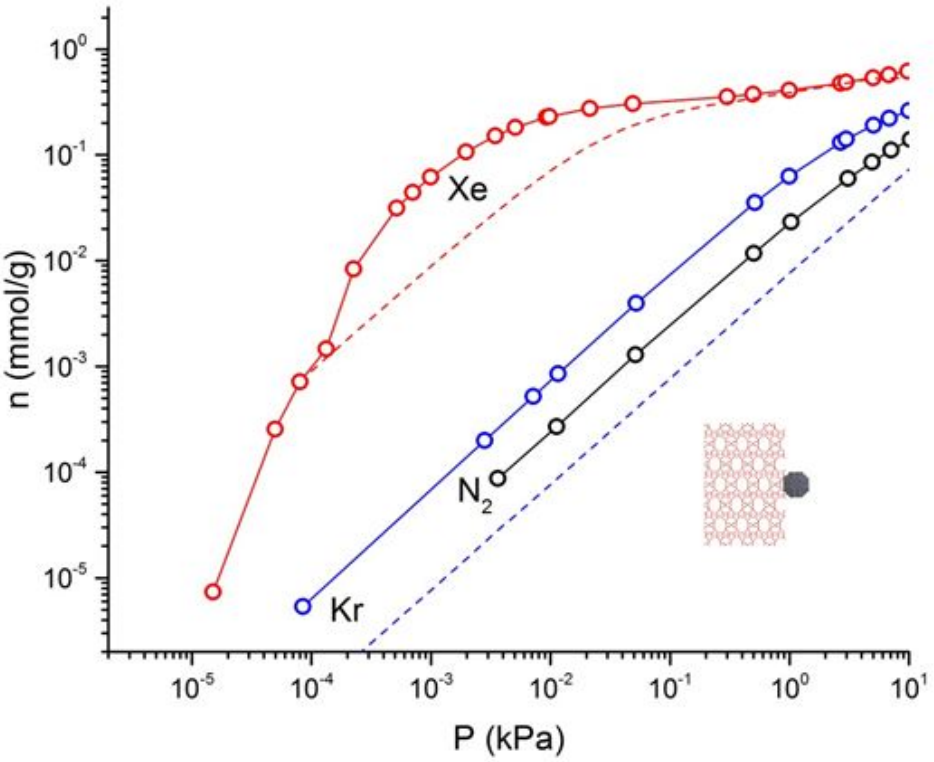

Figure S10. IAST method applied to Xe capture in a mixture of 40 ppm Kr and N2, and to Kr capture in a mixture of 400 ppm Xe and N2, for the Ag@ETS-10 at 298 K. The symbols for the pure adsorption isotherms correspond to the symbols: Xe (O), Kr (O) and N_2 (O). The dashed lines are the adsorption amounts for Xe and Kr as predicted from IAST for the mixture.

Table S2. Determination method of the Henry constants for different adsorption materials.

Adsorbent	Pressure range H_{Kr} (bar)	N	R^2	H_{Kr} (mmol/g/bar)	Pressure range H_{Xe} (bar)	N	R^2	H_{Xe} (mmol/g/bar)	S_H	Ref.
Ni-MOF-74	5.4×10^{-5} – 2.0×10^{-1}	5	0.9196	1.4	4×10^{-6} - 1.5×10^{-1}	5	0.9999	8.4	6	[1,11,20]
CC3	2.6×10^{-2} – 2.5×10^{-1}	9	0.998	1.2	1.4×10^{-2} – 3.9×10^{-2}	3	0.9888	15.5	13	[3,11]
Co-formate	9.3×10^{-3} – 4.0×10^{-1}	10	0.9986	0.9	4.9×10^{-3} – 3.9×10^{-2}	4	0.9965	9.9	11	[5,11]
HKUST-1	2×10^{-3} – 1×10^{-2}	3	0.9545	1.4	2.1×10^{-3} – 1×10^{-2}	3	0.9954	12.2	9	[1,11,21]
SBMOF-1	3.4×10^{-3} – 5.0×10^{-2}	5	0.9905	2.4	6.3×10^{-5} – 1.0×10^{-3}	8	0.9959	38.4	16	[11]
SBMOF-2	1.0×10^{-2} – 5.7×10^{-2}	5	0.9999	1.2	4.2×10^{-2} – 1.1×10^{-1}	5	1	10.4	9	[11,13]
Noria	3.2×10^{-2} – 7.4×10^{-2}	3	0.999	0.9	3.1×10^{-2}	1	-	8.7	9	[11,15]
CA	1.8×10^{-6} - 3.1×10^{-2}			2 (3)	3.0×10^{-7} - 5.0×10^{-4}	6	0.9998	39.1 (2)	20 (3)	†
Ag@ZSM-5	9.5×10^{-8} - 7.7×10^{-6}	4	0.9997	82.5 (4)	7.7×10^{-8} - 4.9×10^{-7}	4	0.8921	2.44×10^{4} (45)	296 (45)	†
					8.8×10^{-2} – 9.8×10^{-2}	2	0.9951	16.6 (47)	0.2 (47)	†
					6.2×10^{-3} – 9.8×10^{-3}	3	0.9223	114.3 (43)	1 (43)	†
					1.4×10^{-6} – 2.9×10^{-6}	2	0.9895	6.97×10^{4} (9)	845 (10)	†
Ag@ETS-10	8.5×10^{-7} - 9.9×10^{-3}	6	0.9999	6.9 (2)	1.5×10^{-7} - 1.3×10^{-6}	4	0.9158	9.86×10^{2} (36)	142 (36)	†
					3.6×10^{-1} – 5.7×10^{-1}	3	0.9212	1.9 (6)	0.3 (6)	†

		$5.2\times10^{-6} – 7.0\times10^{-6}$	2	0.9991	6.17×10^{3} (23)	894 (23)	†

† *This work*

REFERENCES

(1) Liu, J.; Thallapally, P. K.; Strachan, D. Metal–Organic Frameworks for Removal of Xe and Kr from Nuclear Fuel Reprocessing Plants. *Langmuir* **2012**, *28* (31), 11584–11589.

(2) Díaz-García, M.; Mayoral, Á.; Díaz, I.; Sánchez-Sánchez, M. Nanoscaled M-MOF-74 Materials Prepared at Room Temperature. *Cryst. Growth Des.* **2014**, *14* (5), 2479–2487.

(3) Chen, L.; Reiss, P. S.; Chong, S. Y.; Holden, D.; Jelfs, K. E.; Hasell, T.; Little, M. A.; Kewley, A.; Briggs, M. E.; Stephenson, A.; et al. Separation of Rare Gases and Chiral Molecules by Selective Binding in Porous Organic Cages. *Nat. Mater.* **2014**, *13* (10), 954–960.

(4) Tozawa, T.; Jones, J.T.A.; Swamy, S.I.; .Jiang, S.; Adams, D.J.; Shakespeare, S.; Clowes, R.; Bradshaw, D.; Hasell, T.; Chong, S.Y.; Tang, C.; Thompson, S.; Parker, J.; Trewin, A.; Bacsa, J.; Slawin, A.M.Z.; Steiner, A.; Cooper, A.I. Porous organic cages. *Nat. Mater.* **2009**, *8*, 973-978.

(5) Wang, H.; Yao, K.; Zhang, Z.; Jagiello, J.; Gong, Q.; Han, Y.; Li, J. The First Example of Commensurate Adsorption of Atomic Gas in a MOF and Effective Separation of Xenon from Other Noble Gases. *Chem. Sci.* **2013**, *5* (2), 620–624.

(6) Soleimani Dorcheh, A.; Denysenko, D.; Volkmer, D.; Donner, W.; Hirscher, M. Noble Gases and Microporous Frameworks; from Interaction to Application. *Microporous Mesoporous Mater.* **2012**, *162*, 64–68.

(7) Chui, S.; Lo, S.; Charmant, J.; .Orpen, A.; Williams, I. A chemically functionalizable nanoporous material. *Science.* **1999**, *283*, 1148-1150.

(8) Xiao, B.; Wheatley, P.S.; Zhao, X.; Fletcher, A.J.; Fox, S.; Rossi, A.G.; Megson, I.L.; Bordiga, S.; Regli, L.; Thomas, K.M.; Morris, R.E. High Capacity Hydrogen and Nitric Oxide Adsorption and Storage in a Metal-Organic Framework. J. Am. Chem. Soc. **2007**, *129*, 1203-1209.

(9) Farrusseng, D.; Daniel, C.; Gaudillère, C.; Ravon, U.; Schuurman, Y.; Mirodatos, C.; Dubbeldam, D.; Frost, H.; Snurr, R. Q. Heats of Adsorption for Seven Gases in Three Metal−Organic Frameworks: Systematic Comparison of Experiment and Simulation. *Langmuir* **2009**, *25* (13), 7383–7388.

(10) Chowdhury, P.; Bikkina, C.; Meister, D.; Dreisbach, F.; Gumma, S. Comparison of adsorption isotherms on Cu-BTC metal organic frameworks synthetized from different routes. *Microporous Mesoporous Mater*. **2009**, *117*, 406-413.

(11) Banerjee, D.; Simon, C. M.; Plonka, A. M.; Motkuri, R. K.; Liu, J.; Chen, X.; Smit, B.; Parise, J. B.; Haranczyk, M.; Thallapally, P. K. Metal–organic Framework with Optimally Selective Xenon Adsorption and Separation. *Nat. Commun.* **2016**, *7*, ncomms11831.

(12) Plonka, A.M.; Chen, X.; Wang, H.; Krishna, R.; Dong, X.; Banerjee, D.; Woerner, W.R.; Han, Y.; Li, J.; Parise, J.B. Light Hydrocarbon Adsorption Mechanisms in Two Calcium-Based Microporous Metal Organic Frameworks. *Chem. Mater.* **2016**, 28, 1636-1646.

(13) Chen, X.; Plonka, A. M.; Banerjee, D.; Krishna, R.; Schaef, H. T.; Ghose, S.; Thallapally, P. K.; Parise, J. B. Direct Observation of Xe and Kr Adsorption in a Xe-Selective Microporous Metal–Organic Framework. *J. Am. Chem. Soc.* **2015**, *137* (22), 7007–7010.

(14) Tian, J.; Thallapally, P. K.; Dalgarno, S. J.; McGrail, P. B.; Atwood, J. L. Amorphous Molecular Organic Solids for Gas Adsorption. *Angew. Chem. Int. Ed.* **2009**, *48* (30), 5492–5495.

(15) Patil, R. S.; Banerjee, D.; Simon, C. M.; Atwood, J. L.; Thallapally, P. K. Noria: A Highly Xe-Selective Nanoporous Organic Solid. *Chem. – Eur. J.* **2016**, *22* (36), 12618–12623.

(16) Delière, L. PhD Thesis : Adsorption et Séparation Des Gaz Rares Sur Des Adsorbants Dopés À L'argent, Université Claude Bernard - Lyon 1, 2015.

(17) Deliere, L.; Topin, S.; Coasne, B.; Fontaine, J.-P.; De Vito, S.; Den Auwer, C.; Solari, P. L.; Daniel, C.; Schuurman, Y.; Farrusseng, D. Role of Silver Nanoparticles in Enhanced Xenon Adsorption Using Silver-Loaded Zeolites. *J. Phys. Chem. C* **2014**, *118* (43), 25032–25040.

(18) Daniel, C.; Elbaraoui, A.; Aguado, S.; Springuel-Huet, M.-A.; Nossov, A.; Fontaine, J.-P.; Topin, S.; Taffary, T.; Deliere, L.; Schuurman, Y.; et al. Xenon Capture on Silver-Loaded Zeolites: Characterization of Very Strong Adsorption Sites. *J. Phys. Chem. C* **2013**, *117* (29), 15122–15129.
(19) Kuznicki, S.M.; Ansón, A.; Koenig, A.; Kuznicki, T.M.; Haastrup, T.; Eyring, E.M.; Hunter, M. Xenon Adsorption on Modified ETS-10, *J. Phys. Chem. C.* **2007**, 111, 1560–1562.
(20) Thallapally, P. K.; Grate, J. W.; Motkuri, R. K. Facile Xenon Capture and Release at Room Temperature Using a Metal-Organic Framework: A Comparison with Activated Charcoal. *Chem. Commun. Camb. Engl.* **2012**, *48* (3), 347–349.
(21) Hulvey, Z.; Lawler, K. V.; Qiao, Z.; Zhou, J.; Fairen-Jimenez, D.; Snurr, R. Q.; Ushakov, S. V.; Navrotsky, A.; Brown, C. M.; Forster, P. M. Noble Gas Adsorption in Copper Trimesate, HKUST-1: An Experimental and Computational Study. *J. Phys. Chem. C* **2013**, *117* (39), 20116–20126.